

TABLE III: The Same Parameters as in Table I for NaC Solutions

c_M, M	$c_W, g/cm^3$	$s_{max}, \text{\AA}^{-1}$	$d_A, \text{\AA}$	M_A	N_A
0.0299	0.0129	0.063 ± 0.005	110 ± 9	7200	17
0.0697	0.0300	0.087 ± 0.005	79 ± 5	6400	15
0.1411	0.0607	0.105 ± 0.006	66 ± 4	7300	17
0.2504	0.1078	0.122 ± 0.005	57 ± 4	8300	19

NaCDC concentrations, presented in Figure 2 (double rings point), lie nearly on the same curve as in the case of NaDC. Calculated d_A , M_A , and N_A values are presented in Table II. Evidently there is no difference between these two bile salts obtained by X-ray

results.

However, the results for sodium cholate are essentially different. The X-ray scattering maxima for NaC water solution (Figure 6) are more widely spread than in the case of NaDC and NaCDC. For this reason it is difficult to establish their position, s_{max} , with high accuracy. The scattering intensity is about twice lower than for two other bile salts of the same concentration. The calculated d_A , M_A , and N_A values for NaC solutions are presented in Table III. The aggregation number of sodium cholate micelles does not reveal concentration dependence, or if it exists this dependency is very weak.

Chain Packing Statistics and Thermodynamics of Amphiphile Monolayers

I. Szleifer,[†] A. Ben-Shaul,[‡]

Department of Physical Chemistry and The Fritz Haber Research Center for Molecular Dynamics,
The Hebrew University, Jerusalem 91904, Israel

and W. M. Gelbart*^{*,‡}

Department of Chemistry, University of California, Los Angeles, California 90024
(Received: December 4, 1989)

In this paper we extend our earlier theories of chain statistics in amphiphilic aggregates to include the important case of surfactant monolayers. Explicitly, the monomer packing conditions are relaxed to allow for the possibility of nonuniform segment densities. Minimization of the chain free energy is carried out under the constraints of inequalities imposed on moments of the conformational distribution function. Results are presented for the segment density and lateral pressure profiles as a function of area per molecule and chain length. We also discuss the computation of surfactant free energies and their relationship to the successive gas \rightarrow liquid and "expanded liquid" \rightarrow "condensed liquid" phase transitions in adsorbed monolayers at the air/water interface.

1. Introduction

Monolayers of amphiphilic molecules are of interest from both practical and theoretical points of view.¹ Examples of such monolayers are the surfactant films in microemulsions, the (Langmuir) films formed by spreading amphiphilic molecules on a water/air (or water/oil) interface, the dense (Langmuir-Blodgett) films of chain molecules on solid supports, or the two opposing lipid monolayers in biological membranes. Among the major issues concerning the statistical thermodynamic description of these systems are the dependences of chain conformation properties (e.g., segment density profiles) and thermodynamic functions on the average area per chain, the chain length, or the nature of the support and the apolar solvent (oil or air) surrounding the chains. Related questions arise in systems of grafted polymer chains (e.g., on colloidal particles). However, because of the very different chain lengths involved, the theoretical approaches suitable for treating polymer "brushes"² are generally inadequate for treating the relatively short (typically 10-20 segments) amphiphile chains.

In a series of papers we have recently presented a mean-field theory of chain packing statistics in amphiphilic aggregates and applied it to study a variety of systems and phenomena.³⁻⁶ In these studies we have focused on "compact" aggregates, such as surfactant micelles or lipid bilayers in which the hydrocarbon tails of the constituent amphiphiles form a liquidlike hydrophobic core, uniformly packed with chain segments (monomers). For these systems we have calculated various conformation properties, such as bond order parameters and segment spatial distributions,

showing good agreement with the experimental or computer simulation data⁴ whenever comparison is possible. The theory has also been used to calculate thermodynamic functions such as, for example, conformational free energies in pure and mixed aggregates of different geometries^{4,6} or (for the first time from a realistic molecular theory) curvature elastic constants of amphiphilic films.^{5,6} The possibility of applying the theory to systems where the density of chain segments in the hydrophobic region is not necessarily uniform has already been mentioned³ but, so far, has not been explicitly demonstrated. We do so in this paper, with particular reference to amphiphilic monolayers. (The preliminary calculations of monolayer bending constants reported in ref 5b are based on the procedure described in section 2.)

In our treatment of compact aggregates the assumption of uniform segment density in the hydrophobic core is translated into packing constraints (reflecting excluded-volume interactions) on the distribution of chain conformations, which is then derived by minimization of the appropriate free energy functional.³ (An

(1) For a comprehensive recent review, including descriptions of new experimental techniques, see: Knobler, C. M. *Adv. Chem. Phys.* **1989**, *77*, and references therein.

(2) See, e.g.: (a) Milner, S. T.; Witten, T. A.; Cates, M. E. *Europhys. Lett.* **1988**, *5*, 413. (b) *Macromolecules* **1988**, *21*, 2610.

(3) (a) Ben-Shaul, A.; Szleifer, I.; Gelbart, W. M. *J. Chem. Phys.* **1985**, *83*, 3597. See also: (b) *Proc. Natl. Acad. Sci. U.S.A.* **1984**, *81*, 4601. (c) *Physics of Amphiphiles: Micelles, Vesicles and Microemulsions*; Degiorgio, V., Corti, M., Eds.; North-Holland: Amsterdam, 1985; p 404. (d) Ben-Shaul, A.; Gelbart, W. M. *Annu. Rev. Phys. Chem.* **1985**, *36*, 179.

(4) Szleifer, I.; Ben-Shaul, A.; Gelbart, W. M. *J. Chem. Phys.* **1985**, *83*, 3612; **1986**, *85*, 5345; **1987**, *86*, 7094.

(5) (a) Szleifer, I.; Kramer, D.; Ben-Shaul, A.; Roux, D.; Gelbart, W. M. *Phys. Rev. Lett.* **1988**, *60*, 1966. (b) Ben-Shaul, A.; Szleifer, I.; Gelbart, W. M. In *Springer Proceedings in Physics: Physics of Amphiphilic Layers*; Meunier, J., Langevin, D., Boccardo, N., Eds.; Springer-Verlag: Berlin, 1987; Vol. 21, p 2.

(6) Szleifer, I. Ph.D. Thesis, Hebrew University, Jerusalem, 1988.

* To whom correspondence should be addressed.

[†] Present address: Department of Chemistry, Baker Laboratory, Cornell University, Ithaca, NY 14853.

[‡] Also at Institute for Theoretical Physics, University of California, Santa Barbara, CA.

alternative derivation, based on expansion of the many chain partition function, leads to exactly the same distribution.^{3a)} On the other hand, in monolayers, packing constraints set only upper limits on the density profile of chain segments, and the actual profile is an outcome of the minimal free energy procedure. The principles of the derivation are discussed in section 3, and numerical results pertaining to alkyl chains of 8–16 carbons are presented in section 4. In these results we emphasize the dependence of the density and lateral pressure profiles and of the conformational free energy on chain length and head-group area, in the regime corresponding to the liquid state of the monolayer ($\sim 22\text{--}50 \text{ \AA}^2$). This is the region where chain–chain repulsion is significant and where the chains lose conformational entropy as the monolayer is compressed. Both in the theoretical discussion and in the numerical examples we concentrate on a detailed treatment of the conformational free energy and chain statistics of the monolayer. In our derivation of the conformational distribution function, we do not include (or, alternatively, treat as constants) the translational entropy of the chains and the energy of interchain attraction. Accordingly, in a strict sense, our results pertain to monolayers of immobile chains in good (“athermal”) solvents.⁷ The significance of, and the interplay between, these various terms in the monolayer’s free energy are discussed briefly in section 2 and in more detail in section 5.

The theoretical interest in amphiphile monolayers has intensified recently, largely following some important experimental and computational developments. One such development concerns the observation of interesting “super structures” of solid domains (e.g., of spiral, elongated, dendritic, and ordinary rounded shapes) coexisting with a liquid phase, in phospholipid monolayers.^{1,8–10} Different thermodynamic theories have been proposed to explain the phase behavior of these systems.^{11,12} In parallel, several molecular dynamics studies have been concerned with chain packing statistics in the high-density liquid and solid phases of the monolayer.^{13–15} Another important development involves the new experimental evidences supporting the existence of two *first-order* fluid–fluid transitions in Langmuir films: the gas–“liquid-expanded” (G–LE) and the “liquid-expanded”–“liquid-condensed” (LE–LC) transitions.^{1,16,17}

Many theoretical attempts to explain the successive fluid–fluid phase transitions have been reported in the past 15 years, with particular emphasis on the nature of the LE \rightarrow LC transition.^{18–24}

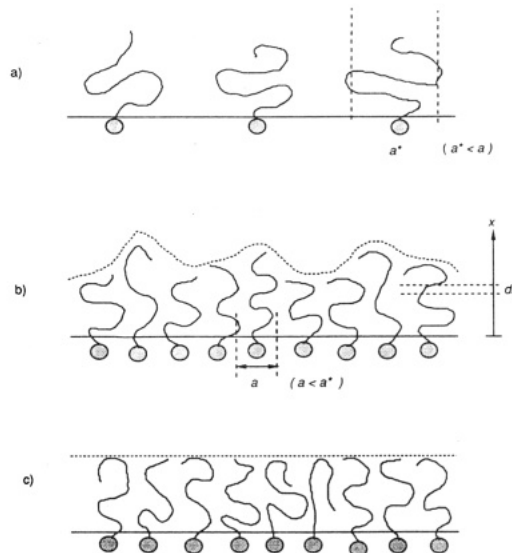


Figure 1. Schematic rendering of amphiphile chains at an air/water or oil/water interface. In (a) the chains are free of one another, occupying an area per molecule a which is significantly greater than the single-chain cross-sectional area a^* . In (b) and (c), on the other hand, a is smaller than a^* , in the case of good and bad solvent, respectively.

Various approaches have been suggested, including several lattice gas (or Ising) type models, involving highly simplified treatments of the conformational degrees of freedom.^{19,20} Recently, two mean-field theories have been presented,^{23,24} in which the coupling between conformational and translational entropies is explicitly considered and chain conformational statistics are treated by using realistic models. Both theories predict the appearance of two successive fluid–fluid phase transitions but attribute them to (apparently) different mechanisms. In section 5, based largely on our present study of amphiphile monolayers, it is argued that these mechanisms are, in fact, qualitatively similar. It should, however, again be emphasized that in our present study we focus only on a detailed description of the conformational statistics of the chains and are not concerned directly with the equation of state (pressure–area isotherm) calculations.

2. Free Energy Considerations

Consider a monolayer of N amphiphiles spread over a total area A of a water/air or water/oil interface, as schematically illustrated in Figure 1. For a given type of amphiphile the conformational and thermodynamic characteristics of the monolayer depend on the average area per molecule, $a = A/N$ ($\sigma = 1/a$ is the surface density), as well as on the temperature and the nature of the nonpolar “solvent” (air or oil) surrounding the amphiphiles’ hydrocarbon tails. The interaction potentials between chain segments, chain segments and solvent molecules, and solvent molecules play a central role in the phase behavior of the monolayer and in the conformational statistics of the constituent chains. In the theory outlined below, the short-range intrachain interactions are treated exactly via explicit counting of all allowed chain conformations, within the framework of the rotational isomeric state model.²⁵ The short-range, excluded-volume, interactions between *different* chains are taken into account through packing constraints reflecting the mean-field potential imposed on each

(7) de Gennes, P. G. *Scaling Concepts in Polymer Physics*; Cornell University Press: Ithaca, NY, 1979.

(8) See, e.g.: (a) Fischer, A.; Sackmann, E. *J. Colloid Interface Sci.* **1986**, *112*, 1. (b) Fischer, A.; Lösche, M.; Möhwald, H.; Sackmann, E. *J. Phys., Lett.* **1984**, *45*, L785.

(9) See, e.g.: (a) Heckl, W. M.; Cadenhead, D. A.; Möhwald, H. *Langmuir* **1988**, *4*, 1352. (b) Kirstein, S.; Möhwald, H.; Shimomura, M. *Chem. Phys. Lett.* **1989**, *154*, 303. (c) Helm, C. A.; Möhwald, H.; Kjaier, K.; Als-Nielsen, J. *Biophys. J.* **1987**, *52*, 381. (d) Flöresheimer, M.; Möhwald, H. *Chem. Phys. Lipids* **1989**, *49*, 231. (e) Miller, A.; Knoll, W.; Möhwald, H. *Phys. Rev. Lett.* **1986**, *56*, 2633.

(10) See, e.g.: (a) Weis, R. M.; McConnell, H. M. *J. Phys. Chem.* **1985**, *89*, 4453. (b) McConnell, H. M.; Moy, V. T. *J. Chem. Phys.* **1987**, *86*, 5852. (11) (a) Keller, D. J.; McConnell, H. M.; Moy, V. T. *J. Phys. Chem.* **1986**, *90*, 2311. (b) McConnell, H. M.; Gaub, H. *J. Phys. Chem.* **1986**, *90*, 1717.

(12) (a) Andelman, D.; Brochard, F.; de Gennes, P. G.; Joanny, J. F. *C. R. Seances Acad. Sci., Ser. C* **1985**, *301*, 675. (b) Andelman, D.; Brochard, F.; Joanny, J. F. *J. Chem. Phys.* **1987**, *86*, 3673.

(13) See, e.g.: (a) Cardini, G.; Bareman, J. P.; Klein, M. L. *Chem. Phys. Lett.* **1988**, *145*, 493. (b) Bareman, J. P.; Cardini, G.; Klein, M. L. *Phys. Rev. Lett.* **1988**, *60*, 2152.

(14) Harris, J.; Rice, S. A. *J. Chem. Phys.* **1988**, *89*, 5898.

(15) Mouritsen, O. G.; Ipsen, J. H.; Zuckermann, M. J. *J. Colloid Interface Sci.* **1989**, *129*, 32.

(16) (a) Pallas, N. R.; Pethica, B. A. *Langmuir* **1985**, *1*, 509. (b) *J. Chem. Soc., Faraday Trans. 1* **1987**, *83*, 585.

(17) Moore, B. G.; Knobler, C. M.; Akamatsu, S.; Rondelez, F. To be published.

(18) For reviews of work published before 1981, see: (a) Bell, G. M.; Combs, L. L.; Dunne, L. *J. Chem. Rev.* **1981**, *81*, 15. (b) Wiegand, F. W.; Kox, A. *J. Adv. Chem. Phys.* **1980**, *41*, 195. (c) Caille, A.; Pink, D.; de Verteuil, F.; Zuckermann, M. J. *Can. J. Phys.* **1980**, *58*, 581.

(19) See, e.g.: (a) Roland, C. M.; Zuckermann, M. J.; Georgallas, A. *J. Chem. Phys.* **1987**, *86*, 5852. (b) Mouritsen, O. G.; Zuckermann, M. J. *J. Chem. Phys. Lett.* **1987**, *135*, 294; *Phys. Rev. Lett.* **1987**, *58*, 389, and references therein.

(20) See, e.g.: (a) Barville, M.; Caille, A.; Albinet, G. *J. Phys.* **1985**, *46*, 101. (b) Legre, J.-P.; Albinet, G.; Firpo, J.-L.; Tremblay, A.-M. *S. Phys. Rev. A* **1984**, *30*, 2720.

(21) Marcelja, S. *Biochem. Biophys. Acta* **1974**, *367*, 165.

(22) (a) Nagle, F. J. *Annu. Rev. Phys. Chem.* **1980**, *31*, 157, and references therein. (b) *Faraday Discuss. Chem. Soc.* **1986**, *81*, 151.

(23) Cantor, R. S.; McIlroy, P. M. *J. Chem. Phys.* **1989**, *90*, 4423, 4431. See also: *J. Chem. Phys.*, in press.

(24) Shin, S.; Wang, Z.-G.; Rice, S. A. Preprint. See also: Popielawski, J.; Rice, S. A. *J. Chem. Phys.* **1988**, *88*, 1279.

(25) Flory, J. P. *Statistical Mechanics of Chain Molecules*; Interscience: New York, 1969.

chain by its neighbors (see below). It has been shown that for chains packed at (nearly) uniform density, such as in lipid bilayers or in micelles, the conformational properties calculated by these approaches are in excellent agreement with experiment and computer simulations.^{3,4}

The inclusion of attractive chain-chain, chain-solvent, and solvent-solvent interactions in our mean-field treatment is possible in different levels of rigor. However, in this paper we ignore them entirely since we focus on systems in which chain-chain and chain-solvent interactions are the same (i.e., chains in a "good" or "athermal" solvent as depicted in Figure 1b). In the language of lattice theories this corresponds to the case where the Flory parameter $\chi = [w_{cs} - (w_{cc} + w_{ss})/2]/kT$ satisfies $\chi \ll 1$; w_{cs} denotes the interaction potential between solvent and chain monomers occupying nearest-neighbor lattice sites, etc. Another limiting case which will be considered for comparative purposes is that of a very poor solvent, corresponding to $\chi \gg 1$. In this limit the system tends to minimize chain-solvent contact resulting (at high surface densities) in the formation of a "compact" monolayer, as schematically depicted in Figure 1.

In addition to interactions with other chain segments and with the molecules of the nonpolar solvent, chain segments interact with the water surface as well. For certain combinations of the interaction potentials w_{cw} , w_{cs} , and w_{sw} (w = water) the chains will preferentially adsorb onto the water surface, whereas less chain-water contact (i.e., repulsion) is expected for other combinations. The incorporation of chain-water interaction in our theory is straightforward, particularly so because this is a single-chain effect. Consequently, as we shall see below, the adsorption energy can be treated as an additive contribution to the conformational free energy per chain, f_c .

In section 5, starting from a general expression for the monolayer's free energy, F , in terms of the multichain distribution function, it is shown that F can be expressed as a sum

$$F = F_c + U - TS_{tr} \approx F_c + U_{rep} + U_{att} + U_{hg} - TS_{tr} \quad (1)$$

Here $F_c = Nf_c$ is the conformational free energy and U is the interamphiphile interaction energy. To a good approximation U can be separated into U_{rep} which accounts for the short-range interchain repulsion, U_{att} which represents the long-range attractive interactions (including the solvent), and a head-group term U_{hg} . S_{tr} is the translational (or "mixing") entropy. The significance of the terms in (1), particularly the separation of the monolayer's entropy into a conformational component which is included in F_c and a translational one in S_{tr} , is discussed in section 5. Now, in order to proceed to the derivation of the conformational distribution function, we focus only on F_c and U_{rep} , treating the other terms as independent of this distribution (as appropriate for an immobile monolayer in an athermal solvent).

3. The Distribution of Chain Conformations

Let $\phi(\alpha, x) dx$ denote the volume occupied by a chain in conformation α in a planar layer of width dx which is parallel to, and at a distance x from, the water/oil (air) interface. The conformations are specified by the coordinates of all atoms (or chain segments) along the chain. For alkyl chains represented by the rotational isomeric state model, $\alpha = b$, ω specifies a given trans-gauche bond sequence, b , and a given overall orientation of the chain with respect to the interface, ω . The chain volume ϕ is conveniently measured in units of v , the (effective) volume of one chain segment in the bulk liquid phase. (For alkyl chains $v \sim 27 \text{ \AA}^3$ is the effective volume of a CH_2 group.) Thus, $\phi(\alpha, x) dx/v = n(\alpha, x) dx$ is the number of (centers of) chain segments of an α chain within x , $x + dx$. $\phi(\alpha, x)$ is proportional to the effective cross-sectional area of the chain at plane x . Note that, for all α , $\int n(\alpha, x) dx = (1/v) \int \phi(\alpha, x) dx = n$ is the number of segments per chain.

For any multichain configuration $\alpha_1, \dots, \alpha_N$ the total area occupied by chain segments at plane x cannot exceed the monolayer's total area A , i.e., $\sum \phi(\alpha_i, x) \leq A$. Multiplying both sides of this inequality by the (normalized) multichain probability

$P(\alpha_1, \dots, \alpha_N)$, summing over all possible configurations $\alpha_1, \dots, \alpha_N$, and dividing by the total number of chains N , we find

$$\langle \phi(x) \rangle = \sum_{\alpha} P(\alpha) \phi(\alpha, x) \leq a \quad (2)$$

Here, $a = A/N$ is the average area per chain and

$$P(\alpha) = \sum_{\alpha_2, \dots, \alpha_N} P(\alpha_1, \alpha_2, \dots, \alpha_N) \quad (3)$$

is the singlet probability distribution of chain conformations (hereafter the "pdc"). In deriving (2), we have used the fact that $P(\alpha_i)$ is the same function for all chains, as appropriate for a single-component monolayer. (The extension of (2) to mixed systems is straightforward.^{4b}) $\langle \phi(x) \rangle$ is the average area taken up by a chain in plane x , which is proportional to the density of chain segments $\rho(x)$ within the planar layer x , $x + dx$, namely $\rho(x) = \langle \phi(x) \rangle / av$. Accordingly, we shall often refer in the following to $\langle \phi(x) \rangle$ as the "segment (or monomer) density profile".

The restriction (2) on the density profile represents the packing constraints imposed on the conformational statistics of a given chain, i.e., on $P(\alpha)$, by its neighbors. As noted earlier, and discussed in more detail elsewhere,³ these constraints are due to excluded-volume (or area) interactions between chains (see also section 5). Thus, eq 2 is a direct consequence of the fact that the term U_{rep} in (1) is either 0 or ∞ : $U_{rep} = 0$ for all allowed, i.e., nonoverlapping, chain conformations; on the other hand, if any two chains overlap (hence (2) is violated) $U_{rep} = \infty$, implying that the corresponding chain configuration is forbidden. The constraint (2) expresses the way in which U_{rep} is coupled to F_c in F .

Many different choices of $P(\alpha)$ can satisfy the inequality (2). But the best approximation to the true pdc is the one which minimizes the singlet ("mean-field") free energy

$$f_c = \sum_{\alpha} P(\alpha) \epsilon(\alpha) + kT \sum_{\alpha} P(\alpha) \ln P(\alpha) \quad (4)$$

subject to the packing constraint (2) and the normalization condition $\sum P(\alpha) = 1$. The first term on the right-hand side of (4) is the average internal energy per chain while the second is equal to $-Ts_c$ with $s_c = -k \sum P(\alpha) \ln P(\alpha)$ being the conformational entropy per chain. In the present context the internal energy includes two terms: $\epsilon(\alpha) = \epsilon_b(\alpha) + \epsilon_a(\alpha)$. $\epsilon_b(\alpha)$ is the energy associated with a given bond sequence, e.g., in the rotational isomeric state scheme $\epsilon_b(\alpha) = n_g(\alpha) e_g$ where n_g denotes the number of gauche bonds along a chain in conformation α and e_g (~ 500 cal/mol) is the gauche energy. $\epsilon_a(\alpha)$ is the adsorption energy which depends on the distances of the various chain segments from the water surface. In the simplest approximation, corresponding to a square well interaction potential of width ξ and depth ψ , we have $\epsilon_a(\alpha) = n_a(\alpha) \psi$, with $n_a(\alpha)$ denoting the number of segments of an α chain located at a distance $x \leq \xi$ from the surface.

For "compact" aggregates such as surfactant micelles or lipid bilayers, in which the density of chain segments is (nearly) uniform throughout the hydrophobic core, the packing constraints (2) are strict equalities, i.e., $\langle \phi(x) \rangle = a$ for all x . (In curved aggregates $a = a(x)$).³⁻⁵ In this case the minimization of f_c subject to $\langle \phi(x) \rangle = a$ is straightforward, yielding

$$P(\alpha) = (1/z) \exp[-\beta \epsilon(\alpha) - \beta \int \pi(x) \phi(\alpha, x) dx] \quad (5)$$

with $\beta = 1/kT$, and the partition function

$$z = \sum_{\alpha} \exp[-\beta \epsilon(\alpha) - \beta \int \pi(x) \phi(\alpha, x) dx] \quad (6)$$

serving as the normalization factor. The $\pi(x)$ are the Lagrange multipliers associated with the packing constraints $\langle \phi(x) \rangle = a(x)$. In other words, $\pi(x)$ is the lateral pressure profile conjugate to the area profile $\langle \phi(x) \rangle$. The numerical values of the $\pi(x)$ are determined by solving the ("self-consistency") equations obtained by substituting (5) back into $\langle \phi(x) \rangle = a$ (for compact planar aggregates). Explicitly, for every value of x we have

$$\sum_{\alpha} [\phi(\alpha, x) - a] \exp[-\beta \epsilon(\alpha) - \beta \int \pi(x') \phi(\alpha, x') dx'] = 0 \quad (7)$$

The solution, $\pi(x)$, satisfies (7) for all x simultaneously. The range of x is the width of the hydrophobic region, i.e., of the order of the length of a fully extended chain, l . In actual computations we discretize the problem by dividing this region into several parallel layers, $i = 1, 2, \dots, L$ of width ΔL (small enough to ensure smooth variation of $\pi(x)$ and $\langle\phi(x)\rangle$). Equation 7 then reads

$$\sum_{\alpha} [\phi_i(\alpha) - \bar{a}] \exp[-\beta\epsilon(\alpha) - \beta\sum_j \pi_j \phi_j(\alpha)] = 0 \quad (\text{all } i) \quad (8)$$

with $\phi_i(\alpha)$ denoting the number of segments of an α chain in layer i , $\bar{a} = a\Delta L/v = \langle\phi_i\rangle$ is the average number of segments in this layer, and π_i is the corresponding lateral pressure.

With the aid of $P(\alpha)$ one can calculate various conformational properties of the chains, e.g., the bond order parameters $\eta_k = \langle P_2(\cos \theta_k) \rangle$, with θ_k denoting the angle between a specific (e.g., C_k-H or C_k-C_{k+1}) bond and a fixed direction in space (typically the normal to the interface); $P_2(x) = (3x^2-1)/2$ denotes the second Legendre polynomial. Similarly, using $P(\alpha)$ we can calculate thermodynamic functions in a mean-field approximation (as implied by the use of a singlet distribution function). In particular, substituting (5) into (4), we get

$$f_c = -kT \ln z + \int \pi(x) \langle\phi(x)\rangle dx \\ = -kT \ln z + \pi_c a \quad (9)$$

where in passing to the second equality we have used $\langle\phi(x)\rangle = a$ and defined the total (conformational) lateral pressure $\pi_c = \int \pi(x) dx$. Using in (9) the explicit form of z from (6), one finds that $\pi(x) = -\partial f_c / \partial \langle\phi(x)\rangle$; i.e., $\pi(x)$ is indeed an area derivative of a free energy. Similarly, using $\partial f_c / \partial a = \int dx (\partial f_c / \partial \langle\phi(x)\rangle) (\partial \langle\phi(x)\rangle / \partial a)$, $\langle\phi(x)\rangle = a$, and the definition of π_c , we find that

$$\pi_c = -\partial f_c / \partial a \quad (10)$$

is the external lateral pressure which must be applied to the monolayer in order to compensate for the loss in conformational free energy associated with chain compression. Note, finally, that since f_c is a Helmholtz free energy, z is not a canonical but, rather, an isothermal-isobaric partition function; i.e., $g_c = -kT \ln z$ is the Gibbs potential per chain.³

The functional form of $P(\alpha)$ for monolayers is similar to the expression given in (5) for compact aggregates. However, several important differences should be noted with respect to the minimization procedure of f_c and the special significance of the inequality in the packing constraint $\langle\phi(x)\rangle \leq a$. Basically, the differences stem from the fact that the state of minimal free energy in monolayers corresponds to a density profile characterized by $\langle\phi(x)\rangle = a$ in certain regions of x and by $\langle\phi(x)\rangle < a$ in others. Furthermore, as we shall see below, $\pi(x) > 0$ for those x values where $\langle\phi(x)\rangle = a$, whereas for $\langle\phi(x)\rangle < a$ we have $\pi(x) \equiv 0$. In other words, $\langle\phi(x)\rangle \leq a$ turns out to be an "irrelevant" (or "redundant") constraint for every x where the $P(\alpha)$ which minimizes f_c yields $\langle\phi(x)\rangle < a$.

To clarify the last statements, let us consider the changes in $P(\alpha)$ as the average area per chain, $a = A/N$, is gradually decreased. Suppose first that the chain density is so low that a is larger than the effective cross-sectional area of a single isolated ("free") chain. Specifically, let $a > \phi(x, \alpha)$ for all α and all x . Then, of course, we also have $a > \langle\phi(x)\rangle_0$ with $\langle\phi(x)\rangle_0 = \sum_{\alpha} P_0(\alpha) \phi(x, \alpha)$ denoting the average area of a free chain at plane x . Clearly, from the definition of a free chain its pdc is $P_0(\alpha) = \exp[-\beta\epsilon(\alpha)]/z_0$, which can also be regarded as a special (low density)—zero lateral pressure—limit of (5). Alternatively, $P_0(\alpha)$ is the pdc which minimizes f_c subject to no packing or other constraints except normalization and impenetrability of the interface. Furthermore, it is not difficult to show⁶ that f_c^0 , the free chain's free energy (obtained by substituting $P_0(\alpha)$ into (4)) is the lowest possible value of f_c . By definition, a relevant constraint on $P(\alpha)$ is a restriction implying $f_c > f_c^0$; otherwise the constraint is irrelevant. Thus if $\langle\phi(x)\rangle_0 < a$, the inequality (2) i.e., $\langle\phi(x)\rangle < a$, is an irrelevant constraint because it is automatically satisfied by $P_0(\alpha)$ which corresponds to the absolute minimum of f_c . Since $P_0(\alpha)$ can be regarded as a special case of (5) with $\pi(x) \equiv 0$, we

can also say that the Lagrange multipliers conjugate to irrelevant constraints vanish identically.

Let x^* denote the "latitude" x where the area profile of the free chain $\langle\phi(x)\rangle_0$ is maximal, with area a^* . As the monolayer is compressed, a point will be reached where $a = a^* = \langle\phi(x^*)\rangle_0$. Slightly beyond this point, when $a = a_1 = a^* - \delta a$, the chains must be squeezed at x^* (within a small region δx^* around this point), in order to satisfy $\langle\phi(x^*)\rangle \leq a_1 < a^*$. Since now $\langle\phi(x^*)\rangle < \langle\phi(x^*)\rangle_0$, it follows that $P(\alpha)$ is different from $P_0(\alpha)$ and, correspondingly, $f_c > f_c^0$. Thus, the constraint (2), $\langle\phi(x)\rangle \leq a$, becomes a relevant one for $x = x^*$ (or, more precisely, for $x = x^* \pm \delta x^*/2$). If $\delta a = a^* - a$ is infinitesimal, we still have $\langle\phi(x)\rangle_0 \leq a$ for $x \neq x^*$; i.e., (2) remains an irrelevant constraint at $x \neq x^*$. Let $P_1(\alpha)$ denote the particular $P(\alpha)$ which minimizes f_c subject to $\langle\phi(x^*)\rangle \leq a_1$. $P_1(\alpha)$ is easily derived by noting the following: (i) For any preassigned value of $\langle\phi(x^*)\rangle$ the $P(\alpha)$ that minimizes f_c is of the (generalized canonical) form from $P(\alpha) \sim \exp[-\beta\epsilon(\alpha) - \beta\pi(x^*) \phi(\alpha, x^*) \delta x^*]$, with $\pi(x^*) > 0$ to ensure $\langle\phi(x^*)\rangle < \langle\phi(x)\rangle_0$. (ii) Substituting (the normalized) $P(\alpha)$ into f_c , we find $\partial f_c / \partial \langle\phi(x^*)\rangle = -\pi(x^*) < 0$. Hence, the lowest free energy price required to satisfy $\langle\phi(x^*)\rangle \leq a_1$ will be obtained for $\langle\phi(x^*)\rangle = a_1$ consistent with our intuitive expectation that $f_c^0 - f_c$ is minimal when the extent of chain distortion, measured by $\langle\phi(x^*)\rangle_0 - \langle\phi(x^*)\rangle$, is minimal. Thus, $P_1(\alpha)$ is given by the canonical functional form above, with the numerical value of $\pi(x^*)$ determined by solving $\langle\phi(x^*)\rangle_1 = \sum P_1(\alpha) \phi(x^*, \alpha) = a_1$.

Upon further decrease in a there will be additional regions of x besides x^* (but still near to it) where the free chain's area exceeds the available area, i.e., regions where $\langle\phi(x)\rangle_0 > a$. (In fact, if $a = a_2 \leq a_1$, we will also have there $\langle\phi(x)\rangle_1 > a_2$, etc.) That is, the range of x over which $\langle\phi(x)\rangle \leq a$ is a relevant constraint increases gradually as the monolayer is compressed. Following similar arguments to those given above, it follows that, for any a , $P(\alpha)$ will be given by the general form (5), with $\pi(x) \neq 0$ only for x where $\langle\phi(x)\rangle = a$. In the other regions $\langle\phi(x)\rangle < a$ is trivially satisfied and $\pi(x) \equiv 0$. It should be noted that the change in the range of x where $\pi(x) \neq 0$, attendant upon a decrease in a , is accompanied by a change in the magnitude of $\pi(x)$ as well.

Finally, a remark should be made regarding a somewhat subtle difference between the evaluation of $\pi(x)$ in monolayers and compact aggregates. In the latter case, we simply solve the coupled equations for all x (more precisely, we solve (8) for all layers i). In the case of a monolayer, on the other hand, one first needs to identify the range of x for which $\langle\phi(x)\rangle = a$ ensures $\langle\phi(x')\rangle < a$ for $x' \neq x$. (In the discretized version, we need to identify the layers i for which the set of constraints $\langle\phi_i\rangle = a$ ensures $\langle\phi_j\rangle < a$ for $j \neq i$.) In general, there is more than one choice (of x region or set of i 's) consistent with this condition. However, only one set of constraints leads to the $P(\alpha)$ which minimizes f_c . Although there is no general algorithm for identifying the desired set of constraints (layers), the practical procedure is quite simple. Basically, we follow the gradual compression pictured above. Namely, starting with $\langle\phi(x)\rangle$ for a free chain we gradually reduce a and note which parts (x values) of the chain must be squeezed as $a \rightarrow a - \delta a$, etc. The lateral pressure profile $\pi(x)$ follows qualitatively the chain distortion profile $\langle\phi(x)\rangle_0 - \langle\phi(x)\rangle$.

4. Results and Analysis

In this section we present some calculations illustrating the conformational statistics of amphiphile chains in monolayers. All the results are for single-chain amphiphiles of the type $H-(CH_2)_{n-1}-CH_3$, with H denoting the polar head group. The head group is treated as a point, marking the chain origin. The chain conformations are represented by the rotational isomeric state scheme,²⁵ with $e_g = 500$ kcal/mol. As in previous calculations,³⁻⁶ we generate for every chain length all the allowed "trans-gauche" bond sequences, b . (By matrix methods²⁶ we calculate the co-

(26) As opposed to assertions elsewhere [Dill, K. A.; Naghizadeh, J.; Marqusee, J. A. *Annu. Rev. Phys. Chem.* **1988**, *39*, 425], we do not count the conformations "by hand" and the chain lengths are not "no longer than about 4-5 segments".

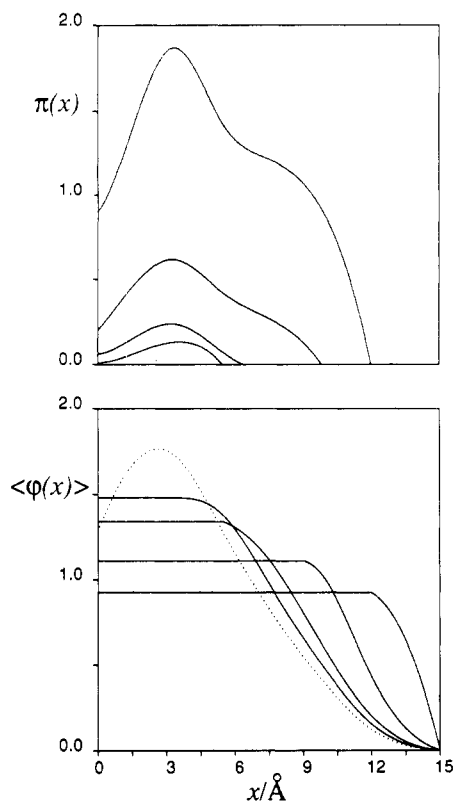


Figure 2. (a) Lateral pressure profile, $\pi(x)$, in units of kT/v , for C_{12} chains at average areas per chain of 25, 30, 35, and 40 \AA^2 . x measures the distance in \AA from the surface. (b) Corresponding $\langle\phi(x)\rangle$'s, in units of $v/\text{\AA} = 27 \text{ \AA}^2$, including that (see dotted curve $\langle\phi(x)\rangle$) for a "free" chain.

ordinates of all chain segments and hence $\phi(\alpha, x)$ for every α .) We exclude all self-crossing conformations by discarding every conformation where any two nonbonded segments are less than 1.5 \AA apart.⁶ Then, for each allowed b we sample a number (usually 36) of overall chain orientations, ω , and head-group positions, x_0 , with respect to the interface. More explicitly, each ω is specified by the set of three Euler angles describing the overall orientation of a chain (with a rigid b), and x_0 is the distance of the head group from the water/oil (air) interface at $x = 0$. (x_0 is randomly chosen within the interval $-\delta x_0/2 \leq x \leq \delta x_0/2$ with $\delta x_0 = 0.75 \text{ \AA}$.) Note that for every b we keep only those ω , x_0 which ensure that all the n chain segments are located on one side of the interface (e.g., $x \geq 0$, or more precisely $x \geq -\delta x_0$). The number of allowed conformations, α , included in the calculation ranges from $\sim 10^4$ for $n = 8$ to $\sim 10^7$ for $n = 16$. It should be stressed, however, that for each chain length the conformations are generated (and classified according to their $\phi_i(\alpha)$) *only once*, the variation with the area per head group of their statistical weights, $P(\alpha)$, being determined by solving (7) or (8) for the appropriate a .

In the calculations below we have chosen $n = 12$ chains as our "standard" example. However, results are also presented for $n = 8, 10, 14$, and 16 carbon chains. It should be remembered that in our chain model the C-C bond lengths is 1.53 \AA and the C-C-C angle is 112.2° , so that the length of a fully extended (all-trans) chain is $l = 1.27 \times (n - 1) \text{ \AA}$ (the H-C bond treated as a C-C bond). Using $v = 27 \text{ \AA}^2$ as the volume of a CH_2 segment, one estimates $a_1 \sim 27/1.27 = 21.2 \text{ \AA}^2$ as the effective cross-sectional area of an all-trans chain. All the areas reported below are calculated relative to this number. As mentioned in section 2, we consider chains in good (apolar) solvents, but we also comment on chain packing in a "compact" monolayer, corresponding to an extremely poor solvent. Some results specifically compare monolayers and bilayers to illustrate the similarity and differences between the two systems.

(a) *Density and Pressure Profiles.* The gradual increase in range and magnitude of $\pi(x)$ associated with decrease in the

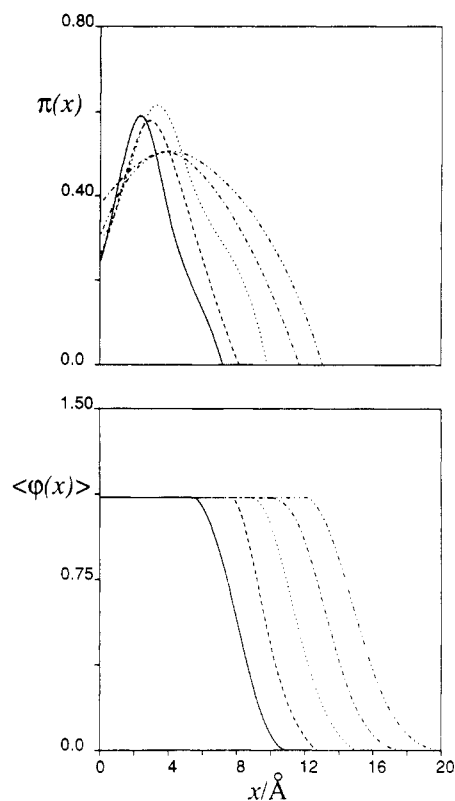


Figure 3. (a) $\pi(x)$ for C_n chains at $a = 30 \text{ \AA}^2$, with $n = 8$ (—), 10 (---), 12 (···), 14 (-·-·-), and 16 (-·-·-), in sample units as Figure 2. (b) Corresponding $\langle\phi(x)\rangle$'s.

average area per chain is illustrated in Figure 2 for 12 carbon chains. Note for example that as the free chain is slightly compressed to $\langle\phi(x)\rangle \leq a_1 = 40 \text{ \AA}^2$, $\pi(x) \neq 0$ for $x \approx 0-4 \text{ \AA}$, which nearly overlaps the region where $\langle\phi(x)\rangle_0 > a_1$, i.e., the region where the free chain must be compressed in order to fit into the given a . The peak in $\pi(x)$ occurs nearly where the extent of chain distortion, $\langle\phi(x)\rangle_0 - a$, is maximal, i.e., at $x \sim 3 \text{ \AA}$ (at the "shoulders" of the chain, near its head group). Similarly, as a falls from $a_1 = 40 \text{ \AA}^2$ to $a_2 = 35 \text{ \AA}^2$, we find, as expected, that $\pi(x) > 0$ in the region where $\langle\phi(x)\rangle_1 > a_2$, etc. Similar correspondence between the pressure and density profiles was found for bilayers as well.²⁷

Consistent with the qualitative analysis in the previous section, we find that for any given a (smaller than $\langle\phi(x^*)\rangle_0$) the density profile $\langle\phi(x)\rangle$ can be divided into two regimes. In the first regime, at low x values (near the "shoulders") the profile is flat; i.e., $\langle\phi(x)\rangle = a$ is constant, the chain is compressed, and $\pi(x) > 0$. In the second regime, mostly reached by segments near the end of the chain, $\langle\phi(x)\rangle$ decreases gradually. In this region the "end" part, or the "tail", of the chain behaves as a free short chain. Of course, the length of this free tail portion depends both on the area, a , and the length, n .

Figure 3 shows $\langle\phi(x)\rangle$ and $\pi(x)$ for a fixed value of a (30 \AA^2) but varying chain length n . Indeed, we see that the ratio between the two regimes of $\langle\phi(x)\rangle$ depends strongly on the chain length. The (nearly) linear variation of the width of each of these regimes can be interpreted as follows. For any given a there is a certain chain length $n = \bar{n}(a)$ such that, for all chains of length $n \leq \bar{n}(a)$, $\langle\phi(x^*)\rangle_0 \leq a$. In other words, for a given area a all chains with $n \leq \bar{n}(a)$ behave as free chains (satisfying $\langle\phi(x)\rangle_0 < a$ for all x —recall that x^* denotes the position for which $\langle\phi(x)\rangle_0$ is maximal). Now consider chains with $n > \bar{n}(a)$. The best way (least free energy price) to pack such chains within area a is to pack the first $n - \bar{n}(a) = n_f$ segments so as to satisfy $\langle\phi(x)\rangle = a$, letting the rest of the chain, i.e., the last $\bar{n}(a)$ segments, behave

(27) Viovy, J. L.; Gelbart, W. M.; Ben-Shaul, A. *J. Chem. Phys.* **1987**, *87*, 4114.

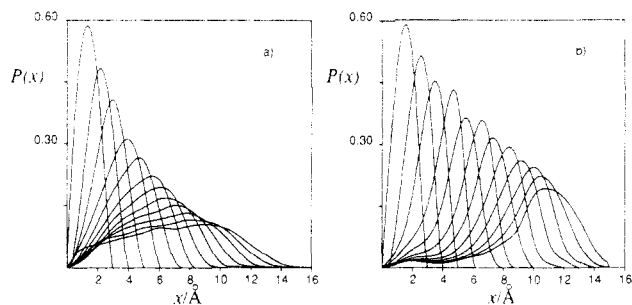


Figure 4. Probability density $P_k(x)$ of finding k th segment of chain at a distance x from the surface, for a "free" C_{12} chain [see (a)] and a constrained C_{12} chain at $a = 30 \text{ \AA}^2$.

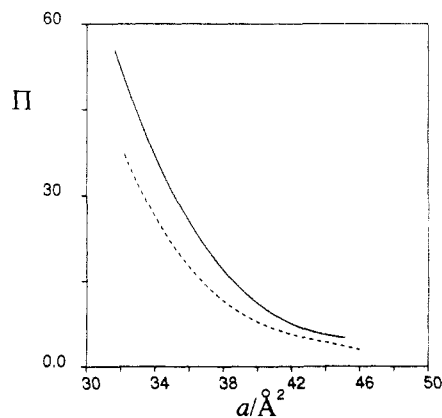


Figure 5. Total (conformational) lateral pressure $\pi_c \equiv \int dx \pi(x)$, as a function of area a , for $n = 16$ (—) and $n = 12$ (---) chains, in units of dyn/cm.

as a free chain. These arguments explain both the linear n dependence of the length of the flat $\langle \phi(x) \rangle$ regime and the very similar shape of $\langle \phi(x) \rangle$ for all n in the second regime.

The qualitative explanation above is only approximate because it implicitly assumes that the two regions of $\langle \phi(x) \rangle$ correspond to two portions of the chain. However, examination of Figure 4 reveals that for the compressed monolayer (Figure 4b) this picture is very reasonable. The figure shows $P_k(x)$, the probability density of finding segment k of the chain at distance x from the interface both for a free chain (a) and for a constrained ($a = 30 \text{ \AA}^2$) chain (b) of length $n = 12$. In both cases $\langle x_k \rangle$, the average distance of segment k from the interface ($x = 0$), increases monotonically with k . Also, in both cases the width, σ_k , of $P_k(x)$ (as measured for example by $\sigma_k^2 = \langle x_k^2 \rangle - \langle x_k \rangle^2$) increases with k as expected from the fact that segments further down the chain can span larger x regimes. Note, however, that the extent of overlap between the x_k 's is considerably smaller for the constrained chain. Again, this behavior is easily understood when we remember that as a decreases the chain is further stretched, implying smaller motional amplitudes for its segments. In particular, in the limit of an all-trans chain $P_k(x) \rightarrow \delta(x - x_k)$ with $x_k \sim k \approx 1.27 \text{ \AA}$.

An idea about the order of magnitude of the total conformational lateral pressures, $\pi_c = \int \pi(x) dx$, is given in Figure 5 which shows π_c as a function of a for $n = 12$ and $n = 16$ chains. These areas, around $35\text{--}45 \text{ \AA}^2$, correspond to the regime where the onset of the LE \rightarrow LC transition typically takes place.^{1,16-24} For each of these areas the conformational free energy as a function of chain length is found to be linear. The linear dependence of f_c on n for a free chain is not surprising. For smaller areas it can be explained following arguments similar to those which we have used to explain the results in Figure 3.

(b) Monolayer vs Bilayer. A bilayer is usually depicted as a "sandwich" of two monolayers facing each other such that their chains form a compact hydrophobic core, uniformly packed with chain segments. Because of the possibility of chain interdigitation across the bilayer's midplane, the chains emanating from the two opposing interfaces interact with each other in the midplane region

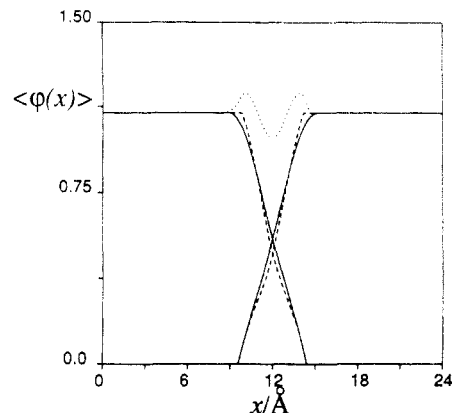


Figure 6. Density profiles, in units of $v/\text{\AA} = 27 \text{ \AA}^2$, for C_{12} chains packed at $a = 29.5 \text{ \AA}^2$ in two interdigitating monolayers (---) and for two opposing C_{12} chains in a bilayer at the same a (—). The dotted curve shows the sum of the monolayer profiles.

(whose relative width increases with the area per chain). Thus, chains in single monolayers and in bilayers need not exhibit the same conformational and thermodynamic behavior. This is particularly so if one compares the behavior of chains in bilayers with those in "compact" monolayers, i.e., monolayers in contact with poor apolar solvents. On the other hand, as we shall presently show, monolayers in contact with good solvents (such as those considered above) closely resemble the monolayers in a bilayer for small chain areas a .

The packing constraint governing chain conformational statistics in a symmetric bilayer is $\langle \phi(x) \rangle + \langle \phi(2L - x) \rangle = a$, with $2L$ denoting the width of the bilayer.³⁻⁶ This equality expresses the requirement for uniform density. (Volume filling requirements imply $L = v/a$ where v is the chain's volume.) The first term accounts for the contribution to the density at x from chains originating at one ($x = 0$) interface, and the second corresponds to the opposing monolayer ($x = 2L$). This equality is also the mathematical expression of the coupling between the two monolayers. Now, recall that for a single monolayer we have required $\langle \phi(x) \rangle \leq a$. Furthermore, we found that $\langle \phi(x) \rangle = a$ over a certain region, say $0 \leq x \leq \bar{x}$, followed by $\langle \phi(x) \rangle < a$ for $x > \bar{x}$. It is not difficult to show that if in a single monolayer $\langle \phi(x) \rangle$ decreases linearly beyond \bar{x} , then simple volume filling considerations imply $\langle \phi(x) \rangle = a[(2L - \bar{x})/2(L - \bar{x})][1 - x/(2L - \bar{x})]$ in this regime. Adding to the density profile of this monolayer an identical profile corresponding to a chain anchored to an opposing monolayer at distance $2L$, we recover the packing condition of the bilayer $\langle \phi(x) \rangle + \langle \phi(2L - x) \rangle = a$. Thus, if $\phi(x)$ decreases linearly beyond \bar{x} , we should expect similar chain statistics in monolayers and bilayers (for the same a).

Examination of Figure 2 reveals that the decrease of $\langle \phi(x) \rangle$ at $x > \bar{x}$ is not exactly linear. Yet a linear dependence is a reasonable approximation for small values of a , in which case the $x > \bar{x}$ region is small and not very significant. (Similarly, for a given a the $x > \bar{x}$ regime is smaller, and the linear approximation for $\langle \phi(x) \rangle$ more appropriate, as n increases; see Figure 3.) Figure 6 shows $\langle \phi(x) \rangle$ for single monolayers of $n = 12$ chains packed at $a = 29.5 \text{ \AA}^2$. It also shows the $\langle \phi(x) \rangle$ corresponding to (each of) the interdigitating monolayers in a bilayer of such chains. The profiles are indeed very similar although clearly not identical. Note that, in particular, the solid curves (bilayer halves) add up to a constant $\langle \phi(x) \rangle = 1.09 (29.5 \text{ \AA}^2)$, whereas the dashed ones (individual monolayers) do not; see dotted curve. Larger differences are expected as a increases and the region of chain interdigitation becomes broader.

Figure 7 shows the C-H order parameter profile of the same chains. Here, as well as in all other conformational and thermodynamic properties, close monolayer-bilayer similarity is observed whenever a is small simply because the monolayers' overlap region is small.

The bilayer's packing constraint $\langle \phi(x) \rangle + \langle \phi(2L - x) \rangle = a$ is obviously more restrictive than the monolayer's constraint $\langle \phi(x) \rangle$

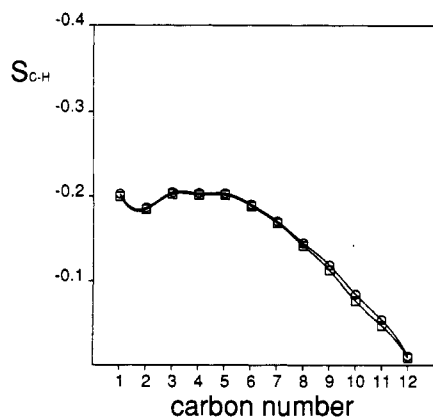


Figure 7. C-H bond order parameter profiles as a function of carbon number for C_{12} chains packed at 29.5 \AA^2 in monolayers (\square) and bilayers (\circ).

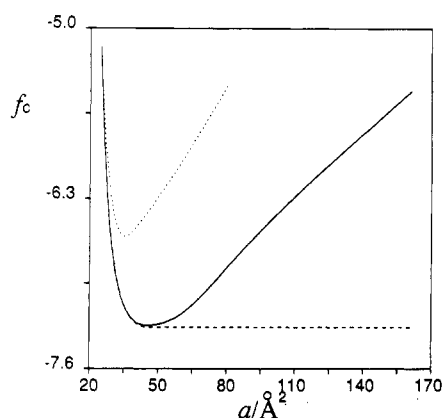


Figure 8. Conformational free energy f_c , in units of kT , for C_{12} chains, packed at different areas per molecule a , in bilayers (—), monolayers (---), and "compact" monolayers (···).

$\leq a$ (because $\langle \phi(2L - x) \rangle > 0$ for all x). Thus, $f_c(\text{monolayer}) \leq f_c(\text{bilayer})$ for all values of a . For small a 's we expect the free energy to be similar, since $\langle \phi(x) \rangle$ [and $P(\alpha)$] is very similar in both cases; cf. Figures 6 and 7. This is quantitatively demonstrated in Figure 8, which shows that $f_c(\text{monolayer}) \leq f_c(\text{bilayer})$ for all $a \geq a^* \sim 45 \text{ \AA}^2$. a^* represents here the same quantity defined in section 3; namely, the chain is conformationally free for all $a \geq a^*$. Consequently, in this regime $f_c(\text{monolayer}) = f_c(a^*) = f_c^0 = \text{constant}$. On the other hand, around $a = a^*$ the bilayer's free energy reaches a minimum, from which it increases as a increases. At the minimum, the chain closely resembles a free chain. The increase in $f_c(\text{bilayer})$ for $a > a^*$ is due to the fact that the chains must be "squashed" (as opposed to the stretching at $a < a^*$) in order to satisfy the packing constraint $\langle \phi(x) \rangle + \langle \phi(2L - x) \rangle = a$. At very large a 's the bilayer is very flat, $L \sim 1/a$, and the chains are essentially two-dimensional. On the other hand, at very small a 's, the chain becomes one-dimensional, i.e., fully stretched (all-trans) and perpendicular to the interface. The scale of f_c in Figure 8 is such that $f_c(a \rightarrow a^* \sim 21 \text{ \AA}^2) = 0$; at this point both the chain entropy and the chain energy are zero.

In Figure 8 we also show f_c for a "compact monolayer". By construction, in this monolayer the density profile is a step function: $\langle \phi(x) \rangle = a$ for $x \leq L$ and $\langle \phi(x) \rangle = 0$ for $x > L$. ($L = v/a$ is the half-width of a bilayer packed with chains at the same area per head group.) This system represents the limit of a monolayer in contact with an extremely poor solvent. The flat chain-solvent interface implied by the step function profile minimizes the unfavorable contact between chain and solvent monomers. We see (Figure 8) that $f_c(\text{compact monolayer}) \geq f_c(\text{bilayer})$ for all areas, the reason being that $\langle \phi(x) \rangle = a$ for $x \leq L$ is a much more stringent constraint than the bilayer's condition $\langle \phi(x) \rangle + \langle \phi(2L - x) \rangle = a$. Apart from serving as a limiting (possibly not very realistic) case of real monolayers, the compact monolayer has

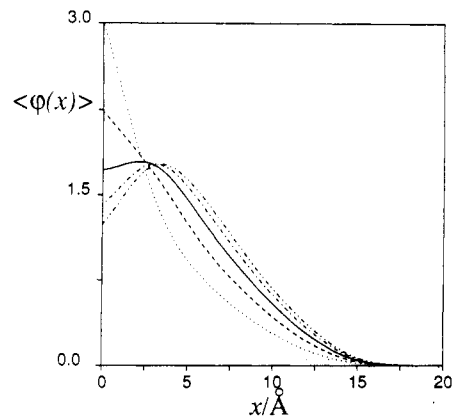


Figure 9. Density profiles of a free C_{16} chain, in units of 27 \AA^2 , for different values of the monomer adsorption energy: $\psi = 0$ (—), $-0.1kT$ (---), $-0.2kT$ (···), $0.1kT$ (-·-), and $0.2kT$ (-·-·).

sometimes been treated in the past as a model for (one half of) a bilayer. The large difference between f_c of the two systems is just one indication of the inadequacy of this model.

(c) *Chain Adsorption.* All the results presented so far in this section correspond to chains that do not interact (attractively or repulsively) with the water interface; i.e., no adsorption energy term $\epsilon_a(\alpha)$ has been included in $\epsilon(\alpha)$. (See discussion following eq 4.) Figure 9 shows the density profile of a free $n = 16$ chain, for different strengths of the adsorption energy. Specifically, for the adsorption energy of a chain in conformation α we use the (square well potential) expression $\epsilon_a(\alpha) = n_a(\alpha)\psi$, where $n_a(\alpha)$ is the number of segments of an α chain at distance $x \leq \xi$ from the interface. For the numerical results in Figure 9 we have used $\xi = 1.0 \text{ \AA}$ (which is simply the width of the first layer, $i = 1$, in the discrete representation of $P(\alpha)$: see, e.g., eq 8).

As expected, negative ψ attracts the chain to the interface, as reflected by the increase in $\langle \phi(x) \rangle$ near $x = 0$. The average adsorption energy is proportional to the number of surface segments, $\langle \epsilon_a \rangle \sim \langle \phi(0) \rangle \psi$. When $\psi/kT \sim -1$, the adsorption energy becomes the dominant factor in f_c^0 and the chain lies essentially flat on the surface. (Note that $\langle \epsilon_a \rangle/kT \rightarrow n\psi/kT \sim -n$ in this case, where n is the total number of chain segments, whereas the entropy loss associated with the passage of a free chain to an essentially 2D chain is $\Delta S \sim nc$ with the constant c smaller than 1.) On the other hand, strong (but short ranged) repulsive interaction will have a small effect on chain statistics. Basically, the result will be a shift of the interface from $x = 0$ to $x = \xi$.

The maximum in the area profile of a free chain occurs always at $x^* \geq 0$, particularly so when the adsorption energy is large. Thus, in practice, the chain is no longer a "free chain" when the monolayer is compressed to areas $a < a^*(\psi) \approx \langle \phi(0) \rangle_0 \approx \langle \phi(x^*) \rangle_0$. Clearly, for all $a < a^*$ the density profile must satisfy the usual packing constraint $\langle \phi(x) \rangle \leq a$ including of course at $x = 0$. Accordingly, the density profile and other conformational properties of the chains are essentially independent of ψ for all $a \leq a^*(\psi)$. The adsorption energy is constant for $a > a^*(\psi)$ and varies (very nearly) linearly with a at smaller areas, because $\langle \epsilon_a \rangle \propto \psi \langle \phi(0) \rangle = \psi a$. Consequently, a constant term $\pi_{ca} = -\partial \langle \epsilon_a \rangle / \partial a = -\psi$ will be included in the conformational lateral pressure of eq 10.

To summarize, segment adsorption can affect the conformational properties of a free chain, such as the density profile and hence, a^* , the area which marks the onset of chain overlap. The dependence of a^* and of π_c on ψ affects, in turn, many details of the phase behavior in amphiphilic monolayers. However, the *qualitative* behavior, such as the number and nature of the transitions, is expected to be independent of ψ (as discussed below in section 5).

5. Discussion and Summary

In section 3 we derived $P(\alpha)$ by minimizing f_c subject to the excluded-area constraint $\langle \phi(x) \rangle \leq a$. In doing so, we have assumed that the other terms in (1) are independent of $P(\alpha)$. In

order to assess the validity and the implications of this assumption, and in order to relate the present work to some recent studies concerning the $G \rightarrow LE$ and the $LE \rightarrow LC$ transitions in amphiphile monolayers, we begin this section by examining the significance of the various terms in the (approximate) free energy expression (1).

Let $P(\alpha_1^N, \mathbf{r}^N)$ denote the probability of finding the monolayer in state $\alpha^N = \alpha_1, \dots, \alpha_N$; $\mathbf{r}^N = \mathbf{r}_1, \dots, \mathbf{r}_N$, with \mathbf{r}_i denoting the position of the head group of chain i and α_i its conformation. The monolayer's free energy is given by

$$F = \int d\mathbf{r}^N \sum_{\alpha^N} P(\alpha^N, \mathbf{r}^N) [\sum_i \epsilon(\alpha_i) + \sum_{i < j} u(\alpha_i, \mathbf{r}_i, \alpha_j, \mathbf{r}_j) + kT \ln P(\alpha^N, \mathbf{r}^N)] \\ = N \sum_{\alpha} P(\alpha) \epsilon(\alpha) + \frac{1}{2} N(N-1) \int \int d\mathbf{r}_1 d\mathbf{r}_2 \sum_{\alpha_1, \alpha_2} P(\alpha_1, \mathbf{r}_1, \alpha_2, \mathbf{r}_2) u(\alpha_1, \mathbf{r}_1, \alpha_2, \mathbf{r}_2) + \\ kT \int d\mathbf{r}^N \sum_{\alpha^N} P(\alpha^N, \mathbf{r}^N) \ln P(\alpha^N, \mathbf{r}^N) = N\langle \epsilon \rangle + \frac{1}{2} N^2 \langle u \rangle - TS \quad (11)$$

As in section 3, $\langle \epsilon \rangle$ is the average (conformational plus adsorption) energy per chain and $P(\alpha) = \int d\mathbf{r}^N \sum_{\alpha_2, \dots, \alpha_N} P(\alpha^N, \mathbf{r}^N)$ is the singlet conformational distribution function. The second term, $u = \frac{1}{2} N^2 \langle u \rangle$, is the total interaction potential in the system, with $u(\alpha_i, \mathbf{r}_i, \alpha_j, \mathbf{r}_j)$ representing the interaction energy between chains i and j . We have assumed here that the interaction potential is pairwise additive; also, to simplify the discussion, we treat the solvent as a continuum. Accordingly, u is in fact a potential of mean force. $P(\alpha_1, \mathbf{r}_1, \alpha_2, \mathbf{r}_2)$ is the pair distribution function defined as usual as the partial sum (integral) of $P(\alpha^N, \mathbf{r}^N)$ over $\alpha_3, \mathbf{r}_3, \dots, \alpha_N, \mathbf{r}_N$. If we separate u into repulsive, attractive and head-group terms, $u = u_{\text{rep}} + u_{\text{att}} + u_{\text{hg}}$, we also have $U = U_{\text{rep}} + U_{\text{att}} + U_{\text{hg}}$, as in eq 1. To a good approximation $u_{\text{hg}} = u_{\text{hg}}(\mathbf{r}_i, \mathbf{r}_j)$ is independent of α_i and α_j . On the other hand, both u_{rep} and u_{att} depend in general on both position and conformation. (Note that for athermal solvents $u_{\text{att}} = 0$ for all conformations, as assumed earlier.)

Exact evaluation of $P(\alpha^N, \mathbf{r}^N)$, hence also of S , is obviously hopeless. One possible alternative is a Flory-Huggins type approximation, as formulated for chain molecules adsorbed on interfaces by Scheutjens and Fleer.²⁸ In very general terms, in this approach, the monolayer is treated by a lattice model and the possible conformations are counted by sequential placements of chains. That is, one first counts the number of ways of placing chain 1 with its head at \mathbf{r}_1 on the surface and with conformation α_1 , then of placing chain 2 given the position and conformation of chain 1, etc. The advantage of this approach is that one treats simultaneously the transitional ("r") and conformational ("α") degrees of freedom. The main disadvantage is that one of the approximations employed is to neglect chain connectivity in the process of state counting. This can lead to serious qualitative problems in the treatment of the monolayer thermodynamics²³ (see also below).

Alternatively, the entropy may be separated into translational and conformational parts. Note, however, that (at least) two separations are possible corresponding to the two decompositions of $P(\alpha^N, \mathbf{r}^N)$, namely, (1) $P(\alpha^N, \mathbf{r}^N) = P(\alpha^N) P(\mathbf{r}^N | \alpha^N)$ and (2) $P(\alpha^N, \mathbf{r}^N) = P(\mathbf{r}^N) P(\alpha^N | \mathbf{r}^N)$, with $P(\mathbf{r}^N | \alpha^N)$ denoting the conditional probability of finding the N chains at positions $\mathbf{r}_1, \dots, \mathbf{r}_N$, given conformations $\alpha_1, \dots, \alpha_N$. $P(\alpha^N | \mathbf{r}^N)$ has the analogous ("opposite") meaning. Thus, the first decomposition yields

$$-\beta S = -\beta(S_c + S_{\text{tr}}) = \sum_{\alpha^N} P(\alpha^N) \ln P(\alpha^N) + \sum_{\alpha^N} P(\alpha^N) \int d\mathbf{r}^N P(\mathbf{r}^N | \alpha^N) \ln P(\mathbf{r}^N | \alpha^N) \quad (12)$$

with $\beta = 1/kT$. A similar expression results from using $P(\alpha^N, \mathbf{r}^N) = P(\mathbf{r}^N) P(\alpha^N | \mathbf{r}^N)$. In both representations the translational part

vanishes identically if the head-group positions are fixed, i.e., if the chains are immobile. The conformational part in (12) becomes identical with (N times) the entropy term in our eq 4, provided that $P(\alpha^N) = P(\alpha_1, \dots, \alpha_N) = P(\alpha_1) \dots P(\alpha_N)$. This of course is the essence of the mean-field approximation. One such scheme has been employed by Cantor and McLroy in their study of the monolayer's equation of state.²³ Following a sequence of approximations they have expressed S_{tr} as a functional of $P(\alpha)$ or more precisely of an effective chain area a_c which depends on the products $P(\alpha_1) P(\alpha_2)$. Then, by minimizing the sum $-T(S_c + S_{\text{tr}}) + u_{\text{att}}$, they derived $P(\alpha)$ and calculated pressure-area isotherms, revealing two successive fluid-fluid transitions. It should be noted that in this theory the effects of chain-chain repulsion enter F via S_{tr} (through its a_c dependence). The general qualitative role of S_{tr} in the phase behavior of fluid supported monolayers, and its a dependence, is discussed again below. Another important term in F which is generally treated via a mean-field approximation is U_{att} . Here, again, the common approximation amounts to replacing $P(\alpha_1, \mathbf{r}_1, \alpha_2, \mathbf{r}_2)$ by $P(\alpha_1) P(\alpha_2) P(\mathbf{r}_1 | \alpha_1) P(\mathbf{r}_2 | \alpha_2)$. The passage from (11) to (1) is then clear, at least formally. $F_c = Nf_c$ is the sum of S_c from (12) and $N\langle \epsilon \rangle$ from the last equality in (11). S_{tr} is the complicated second term in (12), and the potential energy terms correspond to the separation of $\langle U \rangle$ into its three contributions. We have also shown how $P(\alpha)$ is included in both U_{att} and S_{tr} .

We conclude this section with a less formal discussion regarding the roles of F_c , U_{att} , and S_{tr} in the $G \rightarrow LE$ and the $LE \rightarrow LC$ transitions in amphiphile monolayers. Consider first a monolayer of rigid, rodlike molecules. This monolayer may represent a real system of amphiphiles with stiff chains or a hypothetical system of amphiphiles all of which are in the all-trans (or another fixed, "elongated") conformation. In the terminology of the previous sections, the "conformations" $\alpha = b$, ω of these molecules are fully specified by the orientation ω with respect to the surface, because their bond sequence b (all-trans) is the same, i.e., $P(\alpha) \rightarrow P(\omega)$. The phase behavior of such a monolayer of mobile grafted rigid rods has been recently investigated by several groups using different theoretical approaches.²⁹⁻³¹ These studies have established that no first-order phase transition takes place in such a system of hard rods, i.e., rods interacting only through excluded-volume repulsion. (This behavior differs qualitatively from that of hard rods *in bulk*, which exhibit a first-order isotropic-nematic transition.³² The different behavior of the monolayer is directly related to its lower symmetry.³⁰) Furthermore, it has been shown that a single first-order, fluid-fluid, phase transition takes place in the monolayer provided that the interparticle potential includes a (large enough) attractive term. In this transition both the grafting density ($\sigma = 1/a$) and the order parameter, η , which measures the fraction of "upright" rods (or, more precisely, their average alignment) jump simultaneously.^{30,31} Angle-dependent adsorption energy is not a necessary (nor sufficient) condition for a first-order transition.

Since monolayers of "real", i.e., flexible, chains show two successive phase transitions, whereas monolayers of rigid rods show only one transition, it is clear that the additional transition is intimately related to the conformational freedom of flexible chains. Yet, correlating the single transition of the rigid molecules with either the $G \rightarrow LE$ or the $LE \rightarrow LC$ transition of flexible chains is not entirely evident. In fact, by varying the degree of anisotropy of rod-rod interactions, the single transition may resemble more an isotropic-nematic transition which involves a small change in σ and a large one in η or an ordinary 2D gas-liquid transition where the grafting density σ exhibits a large jump while η changes only slightly. In particular, if the interactions (both repulsive and attractive) are completely isotropic, the transition degenerates into a simple 2D gas-liquid transition of rigid, isotropic particles.³¹

(29) Halperin, A.; Alexander, S.; Schechter, I. *J. Chem. Phys.* **1987**, *86*, 6550.

(30) Chen, Z.-Y.; Talbot, J.; Gelbart, W. M.; Ben-Shaul, A. *Phys. Rev. Lett.* **1988**, *61*, 1376.

(31) Wang, Z.-G. *J. Chem. Phys.*, in press.

(32) Onsager, L. *Ann. N.Y. Acad. Sci.* **1949**, *51*, 627.

(28) Scheutjens, J. M. H. M.; Fleer, G. J. *J. Phys. Chem.* **1979**, *83*, 1619; **1980**, *84*, 178.

More generally, any system of adsorbed rigid particles will show a gas-liquid transition provided the attraction between them is strong enough.

At very low densities, when the average area per molecule, a , is considerably larger than the average cross-sectional area of the chain, a^* , a monolayer of (flexible) chains is in fact a 2D gas of free chains. The average shape of the free chain is symmetrical with a caplike (or truncated "blob") envelope whose height decreases as the adsorption energy increases. Although the free chains are not rigid particles, they strongly resist any change in their (average) shape, as this involves (see, for example, Figure 8) a large increase in their conformational free energy, f_c . Thus, unless the external pressure π is large enough, so as to reduce a below a^* , the chains may be treated as (nearly) "rigid blobs". As noted above, a monolayer of such particles can undergo a gas \rightarrow liquid transition if the attraction between the free chain blobs is large enough to compensate for the corresponding loss in translational entropy. Our picture of the G \rightarrow LE transition is that it is, in fact, a gas-liquid transition of free chains, in the course of which the area reduces from some $a_G \gg a^*$ to $a_{LE} \sim a^*$.

Using the terminology of eq 1, we suggest that in the G \rightarrow LE transition U_{att} decreases and $F_{tr} = -TS_{tr}$ increases, while $F_c = Nf_c(a^*)$ remains essentially constant. (The constancy of f_c implies of course that $P(\alpha) = P_0(\alpha)$ is nearly the same in the G and the LE phases.) This qualitative picture is consistent with the recent mean-field theories of Cantor and McLroy²³ and of Shin et al.²⁴ The latter conclude that the G \rightarrow LE involves condensation of the "in surface" portions (i.e., the adsorbed layer) of the amphiphiles, while the former found, following simultaneous minimization of all the terms in (an appropriate form of) F , that the effective excluded area per chain does not change much in the transition. Although the two theories employ rather different chain models and different treatments of translational-conformational coupling, they support the notion that the chains at the coexisting G and LE phases have similar configurations.

When the monolayer is compressed to areas below a^* , the translational motion is largely hindered and, correspondingly, the contribution of S_{tr} to F becomes negligible (and very difficult to calculate). In this regime F_c is no longer constant, as we have discussed in detail in sections 3 and 4. Now, if a second, LE \rightarrow LC, transition takes place, it should involve an interplay between F_c and F_{att} . That is, the loss of conformational freedom should be balanced by increased attraction between neighboring chains. In our discussion in the previous sections we have assumed that $F_{att} = \text{constant}$, as appropriate for chains in athermal solvents. In this case one should not expect another phase transition in the

monolayer and similarly so in "compact" aggregates such as lipid bilayers in which the density is uniform and liquidlike. No phase transition is expected here unless the assumption of constant segment (monomer) density and consequently constant F_{att} is relaxed. This point has been recognized by Marcelja²¹ and Nagle²² over a decade ago in their treatments of the chain melting ("liquid crystal \rightarrow gel") transition in lipid bilayers. In order to predict such a transition, they had to postulate an expression for the decrease of U_{att} with $1/a$.

In the theory of Cantor and McLroy²³ the LE \rightarrow LC transition is associated with the expulsion of solvent molecules from the chain region. In the treatment of Shin et al.²⁴ it is attributed to condensation of the "off-surface" chain portions (whose size increases of course as a decreases). Similarly, in many Ising-type and related "few-state" models, the LE \rightarrow LC transition is reflected by an increase in the fraction of "standing-up" (or stretched) conformations.^{19,20} In the molecular dynamics simulations of Klein et al.¹³ and Harris and Rice,¹⁴ compression of the LC phase is accompanied by enhanced tilt of the alkyl chains and a simultaneous increase in the monomer segment density. In all these approaches, then, the conformational changes are associated with increased attraction energy. Alternatively, they all correspond to an increase in the overall density of chain segments in the hydrocarbon region. Recall that in our treatment in sections 3 and 4, as a decreases below a^* , the height of the $\langle \phi(x) \rangle = \text{constant}$ regime increases gradually. This behavior also implies increasing monomer density and consequently increasing F_{att} upon lowering the area a (for $\chi < 0$).

The qualitative picture emerging from the above analysis is as follows: The G \rightarrow LE transition involves *condensation of (free chain) blobs*, corresponding mainly to a loss of translational entropy ($\Delta S_{tr} < 0$) and a gain in attractive energy ($\Delta U_{att} < 0$) and relatively small change in conformational energy ($\Delta F_c \sim 0$). On the other hand, in the LE \rightarrow LC transition the relevant interplay is between the conformational degrees of freedom, i.e., $\Delta F_c > 0$ (because $\Delta S_c < 0$) and the attractive energy ($\Delta U_{att} < 0$); U_{att} now decreases because the increase in the *monomer* density. S_{tr} plays a minor role in the second transition.

Acknowledgment. This research has been supported by the U.S.-Israel Binational Foundation, the Minerva Gesellschaft für die Forschung (Munich, FRG) at the Fritz Haber Center for Molecular Dynamics, National Science Foundation Grant CHE-88-16059 at UCLA, and National Science Foundation Grant PHY 82-17853, supplemented by funds from the National Aeronautics and Space Administration, at UCSB.